Pakistan Veterinary Journal

ISSN: 0253-8318 (PRINT), 2074-7764 (ONLINE)
DOI: 10.29261/pakvetj/2021.050

RESEARCH ARTICLE

Critical Bone Gap Repair using Autologous Adipose Derived Canine Mesenchymal Stem Cell Graft

Usman Rashid[1], Mansur Abdullah Sandhu[2], Muhammad Yaqoob[1] and Arfan Yousaf[1]*

[1]Department of Clinical Studies, Faculty of Veterinary and Animal Sciences, PMAS-Arid Agriculture University, 46300, Rawalpindi, Pakistan; [2]Department of Veterinary Biomedical Sciences, Faculty of Veterinary and Animal Sciences, PMAS-Arid Agriculture University, 46300, Rawalpindi, Pakistan
*Corresponding author: arfanyousaf@uaar.edu.pk

ARTICLE HISTORY (21-157)

Received:	April 10, 2021
Revised:	June 16, 2021
Accepted:	June 22, 2021
Published online:	July 03, 2021

Key words:
Autologous mesenchymal stem cells
Bone defect
Platelet-rich plasma

A B S T R A C T

Adipose-derived mesenchymal stem cells (AD-MSCs) have been comprehensively reviewed for bone tissue engineering along with different biomaterials. However, the use of canine mesenchymal stem cells (cMSCs) embedded in platelet-rich plasma (PRP) gel can be a novel technique for critical-sized bone defect healing in the canine species. The present study evaluated the infrapatellar fat pad (IPFP) derived MSCs for growth kinetics, expression of CD73, CD90, and CD105 surface antigens, and bi-lineage differentiation along with gene expression studies. Moreover, cMSCs were entrapped in PRP gel (cMSCs-PRP gel) and implanted in 4mm induced radial bone defect. The IPFP-MSCs showed a significantly ($P<0.007$) higher proliferation rate on the 6th and 9th days than on the 3rd day of culture. Furthermore, MSCs harvested from IPFP showed positive expression of CD73, CD90 and CD105 surface antigens. The significant ($P=0.004$) increase in the accumulation of intra-cytoplasmic fat droplets indicated that cMSCs successfully differentiated into adipocytes, while the extracellular deposition of hydroxyapatite minerals and significantly ($P<0.003$) higher alkaline phosphatase (ALP) activity indicates the osteogenic lineage differentiation. Radiographic analysis after transplantation showed that the cMSCs-PRP-gel composite material can fill bone defects quickly compared with the PRP-gel alone. Moreover, the histological analysis of bone gap filled with MSCs-PRP-gel composite exhibited the presence of bony structure as well as osteoblasts and less fibrous tissue. In conclusion, our findings recommend that the cMSCs-PRP gel combination is a suitable choice for the healing of critical-sized bone defect.

To Cite This Article: Rashid U, Sandhu MA, Yaqoob M and Yousaf A, 2021. Critical bone gap repair using autologous adipose derived canine mesenchymal stem cell graft. Pak Vet J. http://dx.doi.org/10.29261/pakvetj/2020.050

INTRODUCTION

Trauma results in various bone defects which are rectified by the formation of new bone in the area through the process of tissue engineering (Deschaseaux *et al*., 2009), depending on age, hormonal, cellular process, and blood supply (Stark, 2013). In the process of tissue engineering, three major components *viz*. cell source, applied cues and matrix are important (Nantavisai *et al.,* 2019). During the repair process, most of the cells are Mesenchymal Stem Cells (MSCs) irrespective of their origin.

For implantation, the application of a proper cell source is necessary for ontogenesis and angiogenesis. Due to tumorigenic properties and cell transplant incompatibilities (Amini *et al.,* 2012) associated with other cell sources, more focus has been directed towards MSCs. The isolation and identification of MSCs from adipose tissue (Jurek *et al.,* 2020), the dental pulp (Tsai *et al.,* 2017), bone marrow (Drela *et al.,* 2020), Wharton's jelly (Kang *et al.,* 2012), synovium and infrapatellar fat pad (IPFP) (Sasaki *et al.,* 2018). The regeneration and differentiation potential of MSCs depends on tissue source, yet to gain the osteogenic trans-differentiation advantage of MSCs cell-to-cell interaction and extracellular mineralization for bone segment development is necessary (Kim *et al.,* 2016).

A dog is known to be the oldest companion animal with physiological and biochemical processes closely related to humans. The implantation of MSCs in canine models is also analogous to human transplantation for exact extrapolation of post-transplantation repercussions (Parker *et al.,* 2010). International Society for Cellular Therapy has

given three distinct characteristics regarding MSCs including plastic adherence ability, expression of CD73, CD90 and CD105 surface markers, and multilineage differentiation ability (Sandhu *et al.,* 2017).

For the successful implantation process major histocompatibility complex type I (MHC-I) and type II (MHC-II) receptors are essential. The MHC-II receptors are located on antigen-presenting cells and play a decisive role in immune tolerance (Bradley, 1991). The absence of type II antigens on MSCs makes them immune-privileged cells. Moreover, human adipose-derived MSCs are more tolerant to immune destruction than bone marrow MSCs (Dela-Rosa *et al.,* 2012).

Tumorous growth, accidental injuries, and congenital defects are major indications for reconstructive orthopedic surgery, and to overcome these imperfections different strategies and materials (bone grafts, calcium phosphorous materials, coral scaffolds, and zinc-based implants) have been applied. This study aimed to test the hypothesis that the combination of autologous platelet-rich plasma (PRP) gel meshwork and IPFP-derived MSCs can reduce the healing time of the critical size bone gap in the canine model.

MATERIALS AND METHODS

Three female Mongrel dogs, aged 6-8 months, with an average weight of 12.5 kg, were kept at the indoor hospital facility of PMAS-Arid Agriculture University, Rawalpindi, Pakistan, (PMAS-AAUR) and provided with commercial dog food (Woof dog food, Pakistan) @ 300g/day and *ad libitum* fresh drinking water. All the animal procedures were approved by the Institutional Animal Ethics committee PMAS-AAUR.

Isolation and multiplication of mesenchymal stem cells: The samples from infrapatellar fat pad (IPFP) were collected under intravenous general anesthesia (ketamine and xylazine @11mg/kg and 2.2mg/kg, respectively). The cMSCs were harvested from the collected samples as described by Sasaki *et al.* (2018). After centrifugation (300*g*; 10 min) the cells were passaged from P0 to P2 in T25 cell culture plastic flasks (Corning, USA) and kept at 37°C with 5% CO_2.

Culture and growth kinetics: At P3 cellular growth kinetics of viable (trypan blue exclusion test) cells/well were counted at day 3, 6, and 9 post-seeding by Neubauer chamber. The population doubling time was calculated by using the following formula (Zhan *et al.,* 2019).

$$PDT = (t \times (\log 2 / (\log Nb - \log Na))$$

Where t is time in days, Nb is the viable cell number and Na is the number of inoculated cell number

Flow cytometric analysis: The expression of CD73, CD90, and CD105 on cMSCs was determined by rabbit raised polyclonal primary antibodies (Elab Science, USA) with 1:100 dilution in Dulbecco phosphate buffer saline (DPBS; Sigma, USA), incubated for 15 min at 37°C, and washed (500*g*; 5min) with DPBS. The Alexa Flour-488 (Invitrogen, USA) conjugated secondary antibodies were diluted in DPBS (1:300) and the cells were incubated for 15 min at room temperature for flow cytometry as detailed by Somal *et al.* (2016).

Bi-linage differentiation: The cMSCs trans-differentiation into adipogenic and osteogenic lineages was induced as previously described by Sandhu et al. (2017) and Jurek *et al*. (2020). Briefly, at P3, the cells were kept in adipogenic/osteogenic transformation medium, comprised of different induction ingredients to make a cocktail. After 7 days, intra-cytoplasmic fat droplets were stained with Oil-Red-O (ORO) and 21 days later, the osteocytes were stained with Alizarin Red S (ARS). The lipid droplets/cell were counted in control and adipocytes by using ImageJ software.

Alkaline phosphatase (ALP) activity: An ALP activity was measured by Elabscience Biotechnology, (Texas, USA), according to the method given by Sangcheshmeh *et al.* (2013). The ALP activity was normalized by the total protein present in the cell lysate.

Gene expression analysis: The cMSCs were tested for expression of gene-specific primer set i.e. *CD73*, *CD90,* and *CD105* fatty acid synthase (*FAS)* and *Osteocalcin.* (Table 1) as specified by Jurek *et al.* (2020). Total RNA was extracted by using TRIZOL reagent (Solarbio, China) and reverse transcribed by a cDNA synthesis kit (Vivantis Technologies, Malaysia). The qPCR reaction was carried out in Galaxy XP Thermal Cycler (Bioer, China) with SYBR green master mix (Thermo Scientific, USA). The cycler reaction was 95ºC for 12 min of initial denaturation, followed by denaturation 95ºC for 15 sec, primer annealing, primer extension at 72ºC for 20 sec, and final hold at 95ºC for 15 sec and normalized to GAPDH.

Preparation of autologous platelet-rich plasma (PRP): For the preparation of PRP the method of Landesberg *et al.* (2000) was used with some modifications. Briefly, 10mL of blood was drawn from the animal with sodium citrate and given a soft spin (101*g*). Subsequently plasma was separated and given a hard to spin (400*g*). The lower one-third portion of plasma was separated aseptically and 10 µL/mL of 20% $CaCl_2$ sterile solution was added along with 3×10^5 autologous cMSCs during the gel formation and kept at 37°C for transplantation.

Table 1: Primer sequences used to amplify specific genes of the canine AD-MSC and differentiated adipocytes and osteocytes

Gene	Sense 5' - 3'	Anti-sense 3' - 5'	Annealing Temp. (°C)	Amplicon size (bp)
CD 73	TTTGGGGAAACCTTTGACC	AGAGGCTCGTAACTGGGTACTC	56.5	116
CD 90	CGGCTTCACCACCAAGGACG	TCTGGGCCAGCAGGCTTATG	53.4	140
CD 105	CCTCAGTGCAAAGAAGAAT	CTTGGAAGATCAGTTTGGGG	55	89
FAS	GGCTGGAGCCGGCTACTGCC	ATTCAGGATGGTAGCGTACA	60	94
Osteocalcin	TGCAACCTTCGTGTCCAAG	TGGAAGCCAATGTGGTCAG	60.5	171
GAPDH	AAGAAGGTAGTGAAGCAGG	GCGTCGAAGGTGGAAGAGTGGG	60	212

MSCs implantation and radiograph analyses: In dogs under general anesthesia, the radius bone was exposed for drilling of two holes (4 mm diameter) ~ 6 cm apart. The proximal and distal holes were implanted with autologous cMSCs-PRP gel and autologous PRP-gel (control), respectively. A series of anteroposterior radiographs (50 kVp and 5mAs) were carried out on days 0, 14, and 28 post-implantation.

Histological analysis: Experimental dogs were euthanized as per American veterinary medical association guidelines (Underwood *et al.,* 2013). The implanted sites were excised, fixed in 4% buffered formalin, and decalcified by using Osteomoll (Merck Millipore, USA). Tissues were dehydrated, embedded in paraffin, sectioned at 5µm thickness, and stained with hematoxylin and eosin to observe cellular changes.

Statistical analysis: The data is presented as mean ± SEM and P<0.05 was taken as significant. Gene expression of *CD73, CD90*, and *CD105* was analyzed by one-way ANOVA. While, lipid droplets/cell, ALP, *FAS* and *Osteocalcin* expression were analyzed by t-test (Sigma Plot 13.0; Systat Software Inc., San Jose, USA).

RESULTS

Identification of cells: After 5 days fibroblast-like cells started forming colonies and expanding outwards. These cells revealed specific growth characteristics, i.e typical spindle shape, plastic adherence, and small vacuole formation as given in Fig. 1A.

Growth kinetics: At P3, the MSCs were evaluated for their proliferation rate at days 3, 6, and 9 as shown in Fig. 1B. Our results showed significant (P<0.007) increase in the proliferation rate at days 6 and 9, as compared to day 3. However, the cell number on day 6 was non-significantly different from that on day 9 of cell culture.

Flow cytometric analysis: The cultured cells were tested for the presence of CD73, CD90, and CD105 for confirmation of cMSCs. Flow cytometric analysis of cMSCs exhibited 46.72% expression of CD73, while the CD90 and CD105 expression remained at 54.86% and 27.65%, respectively, as shown in Fig. 2.

Bi-lineage differentiation potential of cMSCs: In comparison to control cells (Fig. 3A) the transforming adipocytes showed an oval appearance with intracytoplasmic lipid droplets stained red with ORO stain (Fig. 3B). The mean lipids droplets count per cell was significantly (P=0.004) higher in transformed adipocytes as compared to control cells (Fig. 3C). When the cMSCs were kept in an osteogenic induction media, cellular morphology was shifted towards a polygonal-shape as compare to control cells (Fig. 4A). Extracellular mineral deposition islands started appearing after 2 weeks in the induction medium and maximum deposition of extracellular minerals was seen after 3 weeks of induction, as accessed by ARS (Fig. 4B). Osteogenically differentiated cMSCs showed a significant (P<0.003) increase in the ALP activity compared to control cells (Fig. 4C).

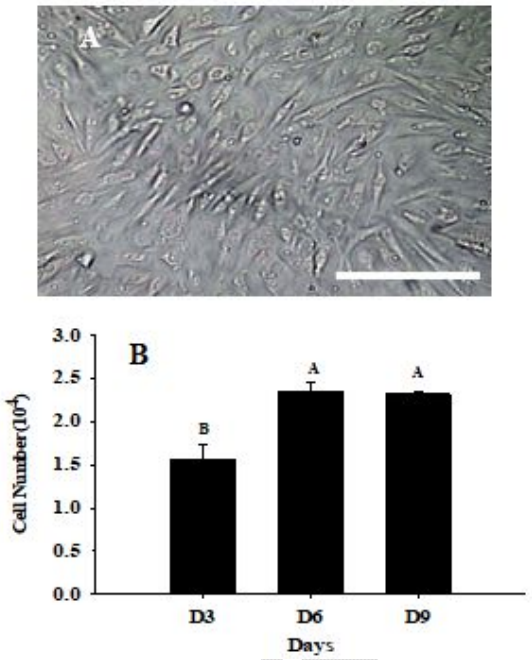

Fig. 1: Spindle-shaped morphology of cultured IPFP derived cMSCs as observed under an inverted light microscope (Magnification 200×). Scale Bar = 15 µm **(A)**: Cellular proliferation (cells × 10^4) at day 3, 6, and 9 **(B)**. Superscript letters $^{A, B}$ show significant difference (*P*<0.007).

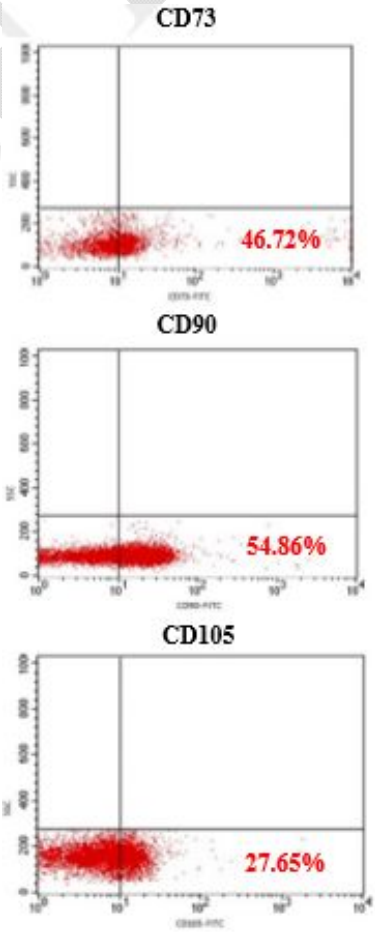

Fig. 2: Flow cytometric expression of CD73, CD90, and CD105 in undifferentiated canine IPFP derived cMSCs.

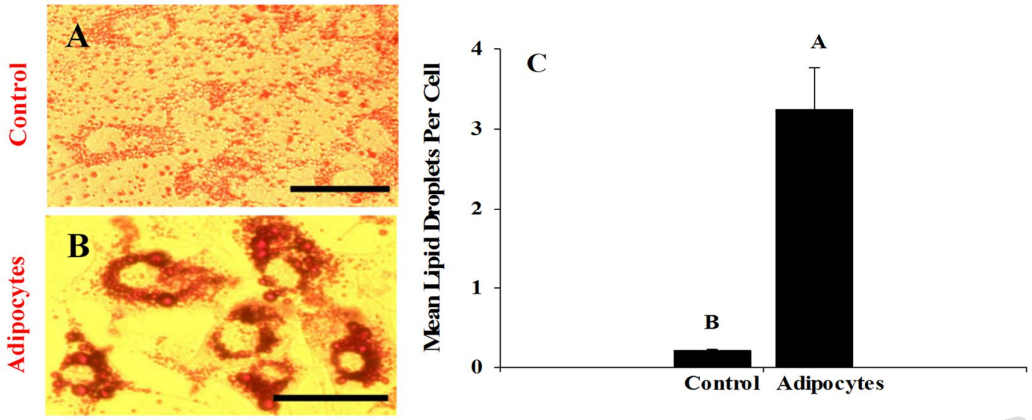

Fig. 3: Adipogenic conversion of IPFP derived cMSCs. Control **(A)** differentiated towards adipocytes and intracytoplasmic fat droplets stained red with ORO stain **(B).** Magnification 400×, scale bar = 20 µm. Mean lipid droplet count per cell in control cells and adipocyte **(C)**. Superscripts [A, B] show significant difference (*P*=0.004).

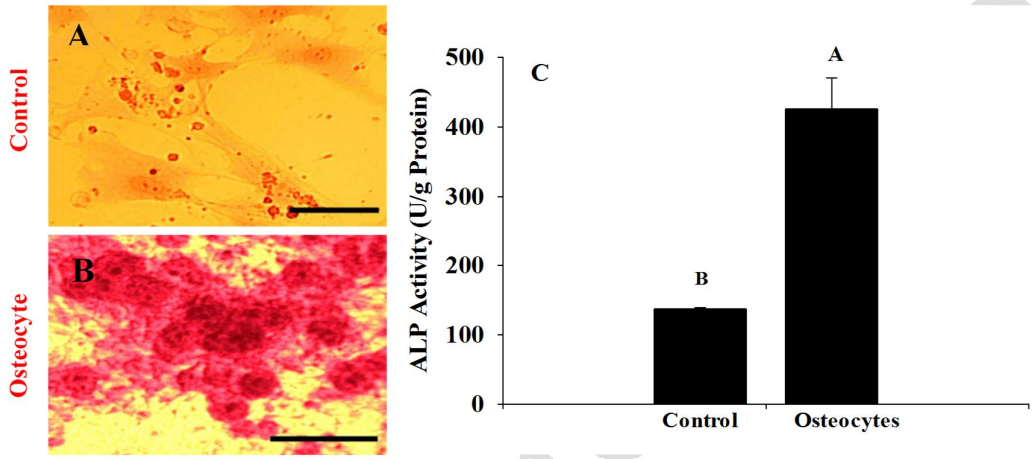

Fig. 4: Osteogenic identification of IPFP derived cMSCs in control **(A)** and differentiated osteocytes with extracellular mineralization stained red with ARS **(B).** Magnification 400×, scale bar = 20 µm. ALP activity (U/g of protein) of control and osteogenic cells **(C).** Superscripts [A, B] show significant difference (P<0.024).

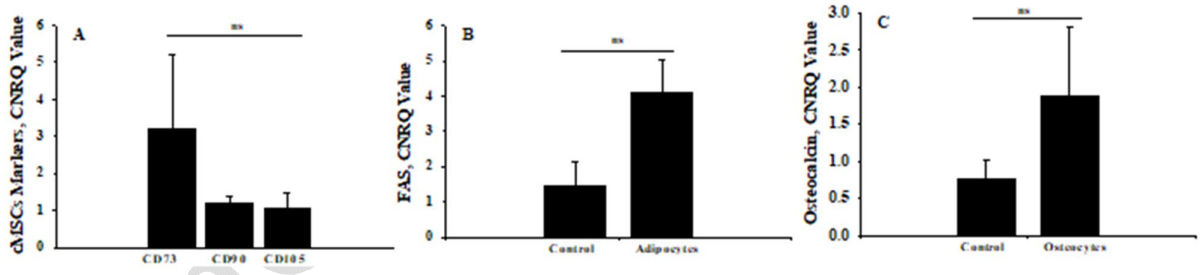

Fig. 5: qPCR analysis of IPFP derived cMSCs in undifferentiated cells for expression of *CD73*, *CD90,* and *CD105* **(A),** the differentiated adipocytes were evaluated for expression of *FAS* **(B),** osteogenically differentiated cell were evaluated for expression of *Osteocalcin* **(C)**.

Gene expression analysis: The qPCR of cultured cMSCs showed the positive expression of *CD73, CD90,* and *CD105*, while, the presence of *FAS* and *Osteocalcin* was non-significantly higher in differentiated adipocytes and osteocytes as compared to control cells, as shown in Fig. 5A-C.

MSCs implantation, radiographic and histological analysis: After implantation of autologous PRP gel (control) and cMSCs-PRP gel in the gaps (Fig. 6A), a serial radiography results revealed that the bone gap implanted with cMSCs-PRP gel showed a robust filling from 14 to 28 days as compared to the gap where only PRP gel was implanted, as shown in Fig. 6 B-D.

After 35 days of implantation, bone gap sections were stained with hematoxylin and eosin stains. The histological presentation of a bone gap filled with MSCs-PRP gel composite showed more bony structure along with the presence of osteoblasts and less fibrous tissue. Whereas, the gap filled with PRP gel alone showed more fibrous tissue and the presence of woven bone (Fig. 7 A&B) which is the indication of delayed healing.

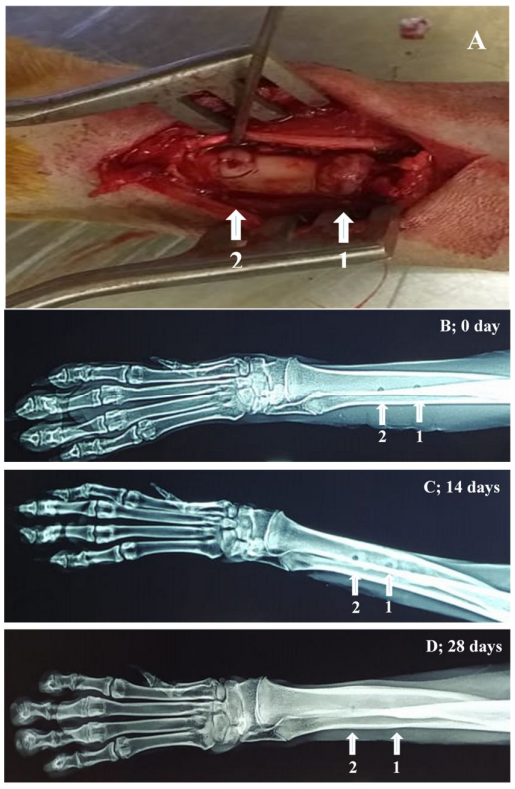

Fig. 6: Surgical implantation of cMSCs-PRP gel composite in proximal **(1)** and PRP gel alone implanted in distal **(2)** holes of (4 mm diameter) radius bone **(A).** Radiographic analysis of the bone gap after implantation of MSCs-PRP gel composite in a proximal hole **(1)** and PRP gel alone in a distal hole **(2)** at day zero **(B)** after 14 days of implantation **(C)** and 28 days of post-implantation **(D)**.

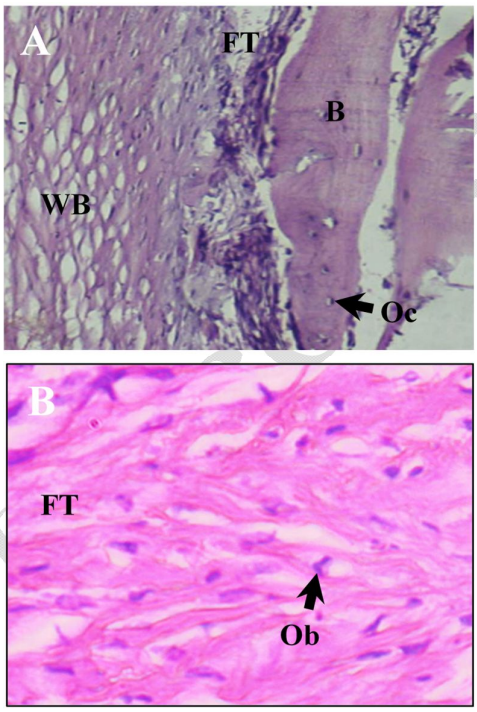

Fig. 7: Histological analysis of bone after 35 days of transplantation. Hematoxylin and eosin-stained sections of the bone. **Panel 1:** PRP Gel alone, **Panel 2:** cMSCs-PRP gel composite. **Abbreviations: WB:** Woven Bone, **B:** Bone, **FT:** Fibrous tissue, **Oc:** Osteocytes, **Ob:** Osteoblasts.

DISCUSSION

It has been shown that the convenience in isolation of AD-MSCs with higher cell yield makes them a favorite choice for researchers. Although cMSCs can be isolated from different body sources, however, IPFP-MSCs have gained popularity because of their higher proliferation rate (Sasaki *et al.,* 2018). Similar results have been achieved in the current study, where IPFP-MSCs showed a significant ($P<0.007$) increase in their proliferation rate at days 6 and 9. In the current study, plastic adherence property and flow cytometric analysis of IPFP-MSCs fulfilled the desired criteria of cMSCs as stated by Dominici *et al.* (2006), and our results are also in line with those observed in bovine (Sandhu *et al.,* 2017) and human (Zuk *et al.,* 2002) AD-MSCs. The cultured cMSCs were further differentiated towards adipogenic and osteogenic lineages. The inability of commonly used adipogenic induction media to induce cMSCs differentiation towards adipocytes has already been reported by Neupane *et al.* (2008). On the contrary, the modified induction media used in our study has successfully differentiated the cMSCs into adipocytes, because the combination of dexamethasone, IBMX, and insulin triggers the activation of *PPARγ*. Moreover, the expression of *FAS* was relatively higher in differentiated adipocytes as compared to control cMSCs, which indicates the increased demand of fatty acids by cells and/or potentiated action of insulin during adipocyte formation (Zhanga *et al.,* 2016).

Alongside adipogenesis, the IPFP-MSCs successfully differentiated towards osteogenic lineage, and extracellular deposited mineral stained positive with ARS stain. The efficient conversion of MSCs to osteocytes in the current study may be the function of dexamethasone supplementation along with β-glycerophosphate, ascorbic acid, and vitamin-D_3. The dose-dependent differentiation of MSCs into adipogenic and/or osteogenic lineages by dexamethasone has also been reported by Gurriaran-Rodriguez *et al.* (2010). The early osteogenic activity (Reddi *et al.,* 2018) was observed in differentiated cMSC and confirmed by significantly ($P<0.024$) higher expression of ALP in differentiated cells compared to control cells. Moreover, the osteogenically differentiated cells showed a higher expression of the *Osteocalcin* gene, during the process of mineralization (Mikami *et al.,* 2007). The fruitful *in vitro* conversion of MSCs into osteogenic lineage has made them a promising choice for implantation. In our study, the radiographic analysis showed a rapid filling of the bone gap implanted with MSCs-PRP gel. The previous studies have also reported bone regenerative properties of MSCs by enhancing the secretion of different growth factors and anti-inflammatory cytokines (Zwingenberger *et al*., 2014). Further, Granero-Molto *et al.* (2009) reported the migration of implanted MSCs via the CXCR4 receptor towards the fracture site hence enhancing the cartilage and bone content of the callus. During tissue injury, immune cells and MSCs share common signaling, migrating, and adhesion molecules including monocyte chemoattractant protein-1 (MCP-1) and chemokine receptor type-2 (CCR2) which enhances MSCs adhesion. The use of PRP gel provides meshwork of fibrin for MSCs anchoring and a source of platelet-derived growth factors (PDGF) as detailed by Lin *et al.* (2017). During *In vitro*

experiment, the formation of new blood vessels is a primary factor to support nutrition for growing and differentiating cells. The rapid filing of the bone gap by cMSCs-PRP gel may be ascribed to the provision of fibrin meshwork and stimulation of neovascularization by MSCs (Kang *et al.,* 2012) that was absent in the control group. Moreover, the continuous proliferation and differentiation of cells resulted in the gap healing in a lesser time compared to the PRP gel treated gap. The efficient reduction in healing time at the site of implantation may be because MSCs or PRP gel both were of the autologous sources, and also MSCs are immune-privileged cells (Arinzeh *et al.,* 2003).

In conclusion, the present study suggests the IPFP is a good source of MSCs, gives a higher number of cells with a fast proliferation rate, and the use of MSCs/PRP gel can reduce the healing time in critical gap fractures.

Authors contribution: This manuscript is based on the Ph.D. thesis of UR. MAS; MY and AY conceived the idea and designed the study. UR conducted the experiments. All authors were involved in data interpretation, write-up, and final approval of the manuscript.

Acknowledgments: We are thankful to Dr. Muhammad Moaeen-ud-Din for extending the laboratory facilities and technical assistance.

Funding statement: This research work was financially supported by HEC-NRPU (7830).

REFERENCES

Amini AR, Laurencin, CT and Nukavarapu SP, 2012. Bone tissue engineering: recent advances and challenges. Crit Rev Biomed Eng 40:363-8.

Arinzeh TL, Peter SJ, Archambault MP, *et al*., 2003. Allogeneic mesenchymal stem cells regenerate bone in a critical-sized canine segmental defect. J Bone J Surg 85:1927-35.

Bradley BA, 1991. The role of HLA matching in transplantation. Immunol Lett 29:55-9.

Dela-Rosa O, Sánchez-Correa B, Morgado S, *et al.,* 2012. Human adipose-derived stem cells impair natural killer cell function and exhibit low susceptibility to natural killer-mediated lysis. Stem Cells Dev 21:1333-43.

Deschaseaux F, Sensébé L and Heymann D, 2009. Mechanisms of bone repair and regeneration. Trends Mol Med 15:417-29.

Drela K, Stanaszek L, Snioch K, *et al.,* 2020. Bone marrow-derived from the human femoral shaft as a new source of mesenchymal stem/stromal cells: an alternative cell material for banking and clinical transplantation. Stem Cell Res Ther 11:1-13.

Dominici MLBK, Le Blanc K, Mueller I, *et al.,* 2006. Minimal criteria for defining multipotent mesenchymal stromal cells. The International Society for Cellular Therapy position statement. Cytotherapy 8:315-17.

Granero-Moltó F, Weis JA, Miga MI, *et al.,* 2009. Regenerative effects of transplanted mesenchymal stem cells in fracture healing. Stem cells 27:1887-98.

Gurriaran-Rodriguez U, Al-Massadi O, Roca-Rivada A, *et al.,* 2010. Obestatin as a regulator of adipocyte metabolism and adipogenesis. J Cell Mol Med 15:1927-40.

Jurek S, Sandhu MA, Trappe S, *et al.,* 2020. Optimizing adipogenic transdifferentiation of bovine mesenchymal stem cells: a prominent role of ascorbic acid in FABP4 induction. Adipocyte 9:35-50.

Kang BJ, Ryu HH, Park SS, *et al*., 2012. Comparing the osteogenic potential of canine mesenchymal stem cells derived from adipose tissues, bone marrow, umbilical cord blood, and Wharton's jelly for treating bone defects. J Vet Sci 13:299-10.

Kim Y, Lee SH, Kang B, *et al*., 2016. Comparison of Osteogenesis between Adipose-Derived Mesenchymal Stem Cells and Their Sheets on Poly-ε-Caprolactone/β-Tricalcium Phosphate Composite Scaffolds in Canine Bone Defects. Stem Cell Int 2016. Article ID:8414715.

Landesberg R, Roy M and Glickman RS, 2000. Quantification of growth factor levels using a simplified method of platelet-rich plasma gel preparation. J Oral Maxillofac Sur 58:297-300.

Lin W, Xu L, Zwingenberger S, *et al*., 2017. Mesenchymal stem cells homing to improve bone healing. J Orthop Translat 9:19-27.

Mikami Y, Omoteyama K, Kato S, *et al*., 2007. Inductive effects of dexamethasone on the mineralization and the osteoblastic gene expressions in mature osteoblast-like ROS17/2.8 cells. Biochem Biophys Res Commun 362:368-73.

Nantavisai S, Egusa H, Osathanon T, *et al*., 2019. Mesenchymal stem cell-based bone tissue engineering for veterinary practice. Heliyon 5:e02808.

Neupane M, Chang CC, Kiupel M, *et al*., 2008. Isolation and characterization of canine adipose-derived mesenchymal stem cells. Tissue Eng Part A 14:1007-15.

Parker HG, Shearin AL and Ostrander EA, 2010. Man's best friend becomes biology's best in show: genome analyses in the domestic dog. Annu Rev Genet 44:309-36.

Reddi S, Shanmugam VP, Tanedjeu KS, *et al.,* 2018. Effect of buffalo casein-derived novel bioactive peptides on osteoblast differentiation. Eur J Nutr 57:593-05.

Sandhu MA, Jurek S, Trappe S, *et al*., 2017. Influence of bovine serum lipids and fetal bovine serum on the expression of cell surface markers in cultured bovine preadipocytes. Cells Tissues Organs 204:13-24.

Sangcheshmeh MA, Shafiee A, Seyedjafari E, *et al.,* 2013. Isolation, characterization, and mesodermic differentiation of stem cells from adipose tissue of camel (Camelus dromedarius). In Vitro Cell Dev Bio-Animal 49:147-54.

Sasaki A, Mizuno M, Ozeki N, *et al*., 2018. Canine mesenchymal stem cells from synovium have a higher chondrogenic potential than those from infrapatellar fat pad, adipose tissue, and bone marrow. PLoS One 13.

Somal A, Bhat IA, Indu B, *et al*., 2016. A comparative study of growth kinetics, in vitro differentiation potential and molecular characterization of fetal adnexa derived caprine mesenchymal stem cells. PLoS One 11.

Stark JG. 2013. Use of selective estrogen receptor modulator for joint fusion and other repair or healing of connective tissue. US Patent 8,501,690.

Tsai AI, Hong HH, Lin WR, *et al*., 2017. Isolation of mesenchymal stem cells from human deciduous teeth pulp. BioMed Res Int 2017. Article ID:2851906.

Underwood W, Anthony R, Cartner S, *et al.,* 2013. AVMA guidelines for the euthanasia of animals: 2013 Ed,Schaumburg, IL: American Veterinary Medical Association.

Zhan X, Ashram S, Luo D, *et al*., 2019. A comparative study of biological characteristics and transcriptome profiles of mesenchymal stem cells from different canine tissues. Int J Mol Sci 20:1485.

Zhanga JS, Leia JP, Weia GQ, *et al*., 2016. Natural fatty acid synthase inhibitors as potent therapeutic agents for cancers: A review. Pharm Biol 54:1919-25.

Zuk PA, Zhu M, Ashjian P, *et al*., 2002. Human adipose tissue is a source of multipotent stem cells. Mol Biol Cell 13:4279-95.

Zwingenberger S, Yao Z, Jacobi A, *et al*., 2014. Enhancement of BMP-2 induced bone regeneration by SDF-1α mediated stem cell recruitment. Tissue Eng Part A 20:810-818.